Escola de Primavera de Transição e Turbulência
Blumenau 2020

ABCM Associação Brasileira de Engenharia e Ciências Mecânicas

12th Spring School on Transition and Turbulence
September 21st-25th, 2020, Blumenau, SC, Brazil

EPTT-2020-0042
ESTIMATION OF THE ENERGY DISSIPATION RATE IN A STIRRED TANK BY 2D PIV MEASUREMENTS

Lucas Freitas de Lima e Freitas
Process Engineering Department, University of Campinas, School of Chemical Engineering
l192527@dac.unicamp.br

Helder Lima de Moura
Process Engineering Department, University of Campinas, School of Chemical Engineering
h115196@dac.unicamp.br

Rodrigo de Lima Amaral
NDF, Department of Mechanical Engineering, POLI, University of São Paulo
rodrigoamaral@usp.br

Paula Trindade da Silva
Process Engineering Department, University of Campinas, School of Chemical Engineering.
p211778@dac.unicamp.br

José Roberto Nunhez
Process Engineering Department, University of Campinas, School of Chemical Engineering.
nunhez@unicamp.br

Guilherme José de Castilho
Process Engineering Department, University of Campinas, School of Chemical Engineering
guijcas@unicamp.br

Abstract. *Stirred tanks agitated by impellers are used in a wide range of industries, e.g., chemical, food, pharmaceutical, and petroleum. The tank design, the impellers, and the number and type of baffles are often associated with their application. Thus, the experimental investigation of these parameters in the turbulent flow is crucial for the control and optimization of this equipment. Particle Image Velocimetry (PIV) is a non-intrusive and quantitative technique that allows determining the vector fields of the flow using tracers. The distribution obtained by this method can also assist in the validation of CFD simulations. The objective of this work is to estimate the energy dissipation rate (EDR) of a stirred tank from PIV 2C-2D measurements and its relation with the spatial resolution. The work was conducted in 0.38 m diameter tank (T) with a pitch blade turbine (PBT) impeller of diameter D ($D/T = 1/3$) in water. The angle-resolved PIV enables a number of turbulent features to be identified. Hence, measurements were taken for three angles, 0°, 45°, and 75°. The EDR was estimated using four methodologies: by the assumption of local axisymmetry (AS), by direct estimation (DE), by modified direct estimation (MDE), and by large eddy simulation (LES). For the optimization and reduction of possible errors, different processing strategies were used to decrease the noise level of the PIV measurements. This study showed that values of EDR were found to vary by two orders of magnitude from near the impeller to the circulation region of the tank. Herein, the effect of measuring angle on EDR was analyzed and provided an insight into the anisotropy of the turbulence in the stirred tank. However, EDR estimation is exceptionally challenging due to the lack of knowledge to distinguish its accuracy and the influence of spatial resolution.*

Keywords: *Turbulence flow, EDR, Spatial Resolution, Stirred tank, Impeller, PIV.*

1. INTRODUCTION

Mechanically agitated mixing tanks are widely used in industrial operations such as in the food, pharmaceutical, oil, chemical, and metallurgical areas. They are used for mixtures of liquids, solid-liquid, dispersion of gas in liquids, reactive flows, and to improve the efficiency of mass and heat transfer (Guida *et al*., 2010). Impellers (or mechanical stirrers) and baffles (or deflectors) are the essential elements of a mixing tank. Due to the application of the mixing tank in different contexts, its geometry, the design of the impellers, and the number of deflectors are important variables in the optimization of this equipment. Thus, these geometric properties and operating conditions can directly define the fluid dynamics inside

the tank (Basavarajappa *et al*., 2015; Sossa-Echeverria and Taghipour, 2015). The flows generated in the agitated tanks are predominantly turbulent due to the high rotor speeds used to achieve the necessary process conditions, such as the mixing time (Basavarajappa *et al*., 2015). Research to investigate the characteristics of turbulent flow in processes is essential for understanding the industrial operations mentioned above. The energy dissipation rate is widely studied to determine the characteristics of the single-phase and multiphase mixing process (Joshi *et al*., 2011; Liu *et al*., 2016). In the turbulent regime, fluid dynamics are characterized by a wide range of length scales, for example, the Kolmogorov scale (Eq. 1) – η, where turbulent kinetic energy is dissipated by molecular viscosity (Escudié and Liné, 2003).

$$\eta = \left(\frac{v^3}{\varepsilon}\right)^{1/4} \tag{1}$$

Where v is the kinematic viscosity of the fluid.

Particle image velocimetry (PIV) is one of the most relevant experimental techniques in contributing to many advances in understanding turbulent and complex flow (Westerweel *et al*., 2013). The PIV technique is a non-intrusive flow measurement method that provides instantaneous velocity fields through tracer particles introduced into the flow (Okamoto *et al*., 2000; Prasad, 2000). According to Hoque *et al*. (2014), it is possible to calculate important parameters such as velocity gradient, integral length scale, structure functions, and spatial energy spectrum from PIV 2C-2D data. However, there are certain conditions to estimate the energy dissipation rate from the velocity data, and each of them has limitations depending on the theoretical assumptions, such as assuming isotropy.

1.1. ENERGY DISSIPATION RATE

In a mixing tank, the impeller transmits kinetic energy to the fluid, generating both the mean flow field and the fluctuating velocities associated with it (Guida *et al.*, 2010). The kinetic energy supplied to the fluid by the impeller is eventually converted to heat by viscous dissipation. Shear stresses perform a deformation work that increases the internal energy of the fluid at the expense of the kinetic energy of turbulence (Khan, 2005). Direct PIV experimental data are unable to resolve the smallest length scale, resulting in underestimation of turbulent dissipation (Hlawitschka and Bart, 2012). In addition, for the PIV 2C-2D technique, only the axial and radial components of the velocity can be measured in the x – y plane (Unadkat, 2009). Thus, several estimation methods have been studied in the past years to decrease the EDR underestimation, and the following methods were performed in this work.

1.1.1. DIRECT ESTIMATION (DE)

Gabriele *et al*. (2009) determined the EDR using direct estimation. For this method, it is necessary to provide an estimate for the third component (w), in this case, using the statistical isotropy hypothesis (Delafosse *et al*., 2011; Gabriele *et al*., 2009; Hoque *et al*., 2015; Khan, 2005; Liu *et al*., 2016; Sharp and Adrian, 2001).

$$\varepsilon_{DE} = v\left[2\overline{\left(\frac{\partial u}{\partial x}\right)^2} + 2\overline{\left(\frac{\partial v}{\partial y}\right)^2} + 3\overline{\left(\frac{\partial u}{\partial y}\right)^2} + 3\overline{\left(\frac{\partial v}{\partial x}\right)^2} + 2\overline{\frac{\partial u}{\partial y}\frac{\partial v}{\partial x}}\right] \tag{2}$$

1.1.2. MODIFIED DIRECT ESTIMATION (MDE)

According to Alekseenko *et al.* (2007), another method to estimate the EDR is using a correction factor. The proposed correction factor, f_e based on Pao (1965) spectrum for PIV resolutions below the Kolmogorov length scale, as follow:

$$f_e = 1 - e^{\left[-\frac{3}{2}\alpha\left(\frac{\pi}{\Delta}\eta_M\right)^{4/3}\right]} \tag{3}$$

$$\eta_M = \left(\frac{v^3 f_e}{\varepsilon}\right)^{1/4} \tag{4}$$

$$\varepsilon_{MDE} = \varepsilon_{DE}/f_e \tag{5}$$

Where α is a constant equal to 1.6, η_M is the modified Kolmogorov length scale and ε_{MDE} was computed iteratively as follows: in the first cycle, f_e was taken as unity, and the value of η_M was estimated from the hypothetical value of ε, where $\varepsilon = max(\varepsilon_{MDE})$. In the second cycle, f_e was calculated from Eq. (3), and η_M was recalculated.

1.1.3. LARGE EDDY SIMULATION (LES)

The energy dissipation rate can be estimated by the large eddy simulation. Sheng *et al.* (2000) proposed this method that estimates the EDR by multiplying the sum of terms known by $9 / 5$. Consequently, velocity gradients should be replaced by the sum of the known terms multiplied by $12 / 6$. Thus, the estimation of EDR by the LES method is given by:

$$\varepsilon_{LES} = C_s^2 \Delta^2 \left[4 \overline{\left(\frac{\partial u}{\partial x}\right)^2} + 4 \overline{\left(\frac{\partial v}{\partial y}\right)^2} + 2 \overline{\left(\frac{\partial v}{\partial x}\right)^2} + 2 \overline{\left(\frac{\partial u}{\partial y}\right)^2} \right]^{3/2} \quad (6)$$

Where Δ is the filtered scale corresponding to the size of the interrogation window used in the PIV and C_s is the Smagorinsky constant, which can be assigned a value equal to 0.21 (Meyers and Sagaut, 2007).

1.1.4. ASSUMPTION OF LOCAL AXISYMMETRY (AS)

This method to estimate the EDR is an alternative way, depending only on the measurements in the x – y plane. Once the asymmetric axis is identified, this hypothesis leads to an estimate of the EDR using the four velocity gradients solved in the 2D Classic PIV (George and Hussein, 1991; Xu and Chen, 2013). Thus, EDR can then be estimated from the velocity gradients of the measured planes using the Eq. 2.

$$\varepsilon_{AS} = v \left[-\overline{\left(\frac{\partial u}{\partial x}\right)^2} + 8 \overline{\left(\frac{\partial v}{\partial y}\right)^2} + 2 \overline{\left(\frac{\partial v}{\partial x}\right)^2} + \overline{2 \left(\frac{\partial u}{\partial y}\right)^2} \right] \quad (7)$$

2. METHODOLOGY

Experiments were conducted in an acrylic tank with ASME 10% torispherical bottom (width $T = 380\ mm$, height $H = 760\ mm$ ($50\ L$)) equipped with a four pitched-blade impeller (diameter $D = T/3$ and inclination angle 45°) and four equally spaced baffles ($B = 0{,}1\ T$), as shown in Fig. 1. The chosen fluid for the experiments was water with the following physical properties density $\rho = 998.2\ kg \cdot m^{-3}$, and viscosity $\mu = 1.003\ mPa \cdot s$. The impeller was placed, and its rotation speed was maintained at $N = 660\ rpm$, providing a Reynolds number $Re = \rho N D^2/\mu$ (230,000). As shown in Fig. 1(a), the PIV 2C-2D system consists of a Nd:YAG laser (emission wavelength $532\ nm$), a FlowSense EO 8M-21 CCD camera with a resolution of 3312 × 2488 pixels. The seeding particles used were silver coated hollow glass spheres with a mean particle diameter of 10 µm provided by Dantec Dynamics. A shaft encoder was employed to control the camera and laser by impeller position. In the present work, the angle between the impeller blade and the measuring plane was set to 0°, 45°, and 75° to demonstrate the anisotropy of flow in the stirred tank. The angle-resolved (AR) measurements were performed considering a fixed position between two consecutive baffles, and varying the plane relative to the position of the impeller, considering the 0° starting point in this plane. In other words, the tip of the impeller was aligned at 0° relative to the 45° plane between two baffles.

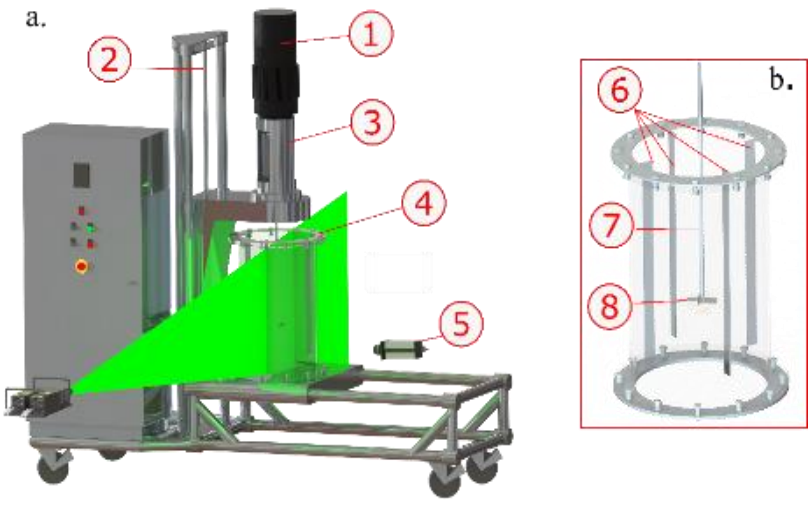

Figure 1: Experimental set-up for PIV investigation: 1. Motor; 2. Shaft for adjusting the impeller height; 3. Torquemeter; 4. Acrylic tank; 5. Camera; 6. Baffles; 7. Shaft; 8. PBT 45° impeller.

For each experiment, 1,000 pairs of images were recorded in double-frame mode and $100\,\mu s$ interframe time. The initial spatial resolution was defined as 36 × 36 px with a value of the size of the interrogation window (Δ) equal to 1.08 mm and with a final resolution of 5 × 5 px with a window size corresponding to 0.15 mm. In the image processing, the multigrid iterative interrogation window deformation strategy was applied, which was carried out from the adaptation of the spatial resolution (Kim and Sung, 2006). In this way, the size of the interrogation window was reduced progressively in 5 steps, making it possible to obtain 6 different spatial resolutions to analyze the EDR distribution: 36 × 36 px (1.08 mm), 27 × 27 px (0.810 mm), 20 × 20 px (0.6 mm), 15 × 15 px (0.45 mm), 10 × 10 px (0.3 mm) and 5 × 5 px (0.15 mm). Images were processed with standard cross-correlation (SCC) technique and optimized using the signal-to-noise ratio (SNR) metrics. The experiments were carried out with the camera focused on a limited image area to obtain high spatial resolution levels. Thus, the main objective of this study was to analyze the effect of estimating the EDR values from the variation of the spatial resolution for different fixed positions of the impeller in the image plane (0°, 45°, and 75°) in angle-resolved measurements. To observe this effect, 4 methods of estimating EDR, described above, were studied, namely: local axisymmetry (AS), direct estimation (DE), modified direct estimation (MDE), and large eddy simulation method (LES).

3. RESULTS AND DISCUSSION

Figure 2 shows the results of the EDR distribution obtained at AR 0 ° measurements in two spatial resolutions: 36 × 36 px (1.08 mm) and 10 × 10 px (0.3 mm). The EDR distribution was estimated by the four methods described in the introduction, considering the EDR normalized by the rotation speed (N) and tank diameter (D), in the relation: ε/N^3D^2. The results for the 36 × 36 px resolution showed that the normalized EDR values varied in a range from 0 to 0.15 for the AS, DE, and MDE methods, whereas for the LES method, the maximum normalized EDR value was equal to 4. For the EDR distribution obtained for the 10 × 10 px of spatial resolution, the values of the maximum ε/N^3D^2 increased by 85% for the first 3 methods, with a value equal to $\varepsilon/N^3D^2 = 1$, while for the LES method, the increase in ε/N^3D^2 between the two spatial resolutions was smaller – with 20% variation compared to 36 × 36 px. It is evident the increase of the spatial coherence in the ε/N^3D^2 distributions by varying the spatial resolution from 1.08 mm to 0.3 mm. Also, the turbulent kinetic energy dissipation initialized just above the impeller tip and concentrated in that region for both spatial resolutions at AR 0°. While far from this region, little variation in energy dissipation was observed. This behavior is related to the formation and dissipation of the trailing vortex behind the reference blade, which occurred from this angle in a circulatory movement through the interaction of the impeller blades with the baffles, as described by Schäfer *et al.* (1998). In other words, a significant change in velocity caused by the movement of the blades occurred in this region close to the impeller, which generated considerable energy dissipation just behind and above the lead blade at AR 0°. Besides, the turbulence treatment was performed using an angle-resolved approach; thus, the periodicity induced by the crossing of the blades was attenuated, so that the dissipation values found have a main random contribution, in other words, the intrinsic turbulence to the flow (Yianneskis, 2000).

Figures 3 and 4 show the distribution of ε/N^3D^2 estimated by the same methods and spatial resolutions, at AR measurements 45° and 75°, respectively. Analyzing Fig. 3 for the 45° AR, it was possible to observe deviations from the maximum values of ε/N^3D^2 related to the effect of increasing the spatial resolution for the AS, DE and MDE method, whose value was increased in 87.5%, with local maximum equal to $\varepsilon/N^3D^2 = 0.4$. While for the LES method, the increase in spatial resolution to 0.3 mm implied an increase of 46.67% in the maximum of ε/N^3D^2, with a value equal to $\varepsilon/N^3D^2 = 1.5$. Applying the same analysis to Fig. 4, the deviations from the maximum of ε/N^3D^2 for the three methods were around 90%, with a final value $\varepsilon/N^3D^2 = 0.25$ for AS and DE, while for the MDE method, the final value was equal to $\varepsilon/N^3D^2 = 0.3$. The variation at AR 75° for LES was 50%, with a final value equal to $\varepsilon/N^3D^2 = 0.6$.

It was observed the increase of AR leads to a high deviation between the local maximums of EDR. This may be related to a higher degree of anisotropy for greater angles associated with the effect of magnifying the spatial resolution. Higher spatial resolutions imply a more significant number of velocity vectors computed in the plane optimizing the representativeness of ε/N^3D^2 – predominantly anisotropic regions that present different turbulence scales (Micheletti *et al.*, 2004; Liu *et al.*, 2016). This can be evidenced by the points with intense magnitude (in red) of ε/N^3D^2, possibly inadequate in terms of representativeness of the phenomenon, for the 36 × 36 px resolution in the impeller discharge region. These inappropriate points occurred for both 45° and 75° angles in the vortex region of the PBT 45° impeller. This region is characterized by a non-stationary flow, with recirculation, vortices, eddies and pseudo turbulence (periodicity) that can be related to different macro instability phenomena (Hasal *et al.*, 2008).

Still comparing the dissipation phenomenon for different angles, from a global perspective, it was possible to observe for all ARs, a region of high energy dissipation presented itself close to the impeller tip. Also, it was clear that the maximum point shifted in the measurement plane, as the impeller blade changed its angle, indicating the movement and dissipation of the trailing vortices in the discharge region, suggesting a helical circular shape (Schäfer *et al.*, 1998; Roy *et al.*, 2010). Comparing the 0°, 45° and 75° angles, the maximum points ε/N^3D^2 reduced proportionally with the increase of the blade angle. This indicated that the dissipation of the vortices occurred in a small region and gradually with the movement of the impeller relative to the baffle. It was also possible to observe that at AR 45°, the maximum point occurred

farther from the tip of the impeller, indicating that for this angle, significant axial extension of the dissipated trailing vortices occurred.

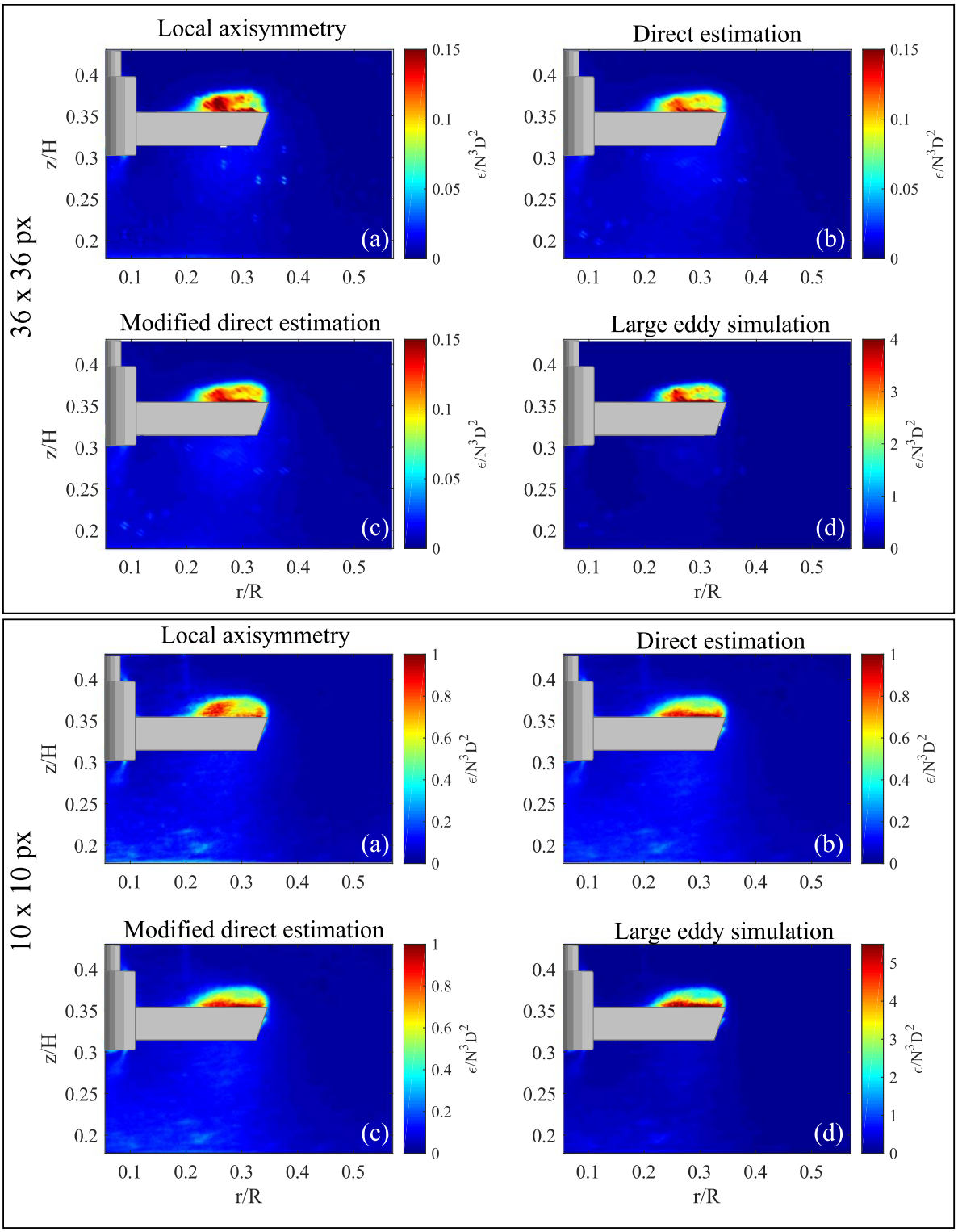

Figure 2: Angle-resolved EDR distribution of 0° using different estimation methods with 36 × 36 px or 10 × 10 px (a) AS; (b) DE; (c) MDE and (d) LES.

At AR 75°, however, it was possible to observe a greater spread of the dissipation in the impeller discharge region, because, at this angle, there was greater interaction between the trailing vortex formed with the bulk flow, with a mixture between high and low ε/N^3D^2. This phenomenon described the dispersion, in which the vortices produced near the impeller blade broke as these structures move from the tip to the region of strong turbulence, where friction with the fluid

dissipated most of the energy (Yianneskis, 2000; Ducci and Yianneskis, 2007). The understanding of this mixing process and the characterization of these macro instabilities defined by trailing vortices and their effect on the efficiency of the agitation processes are complex and still presents study opportunities, as mentioned by Nikiforaki *et al.* (2003).

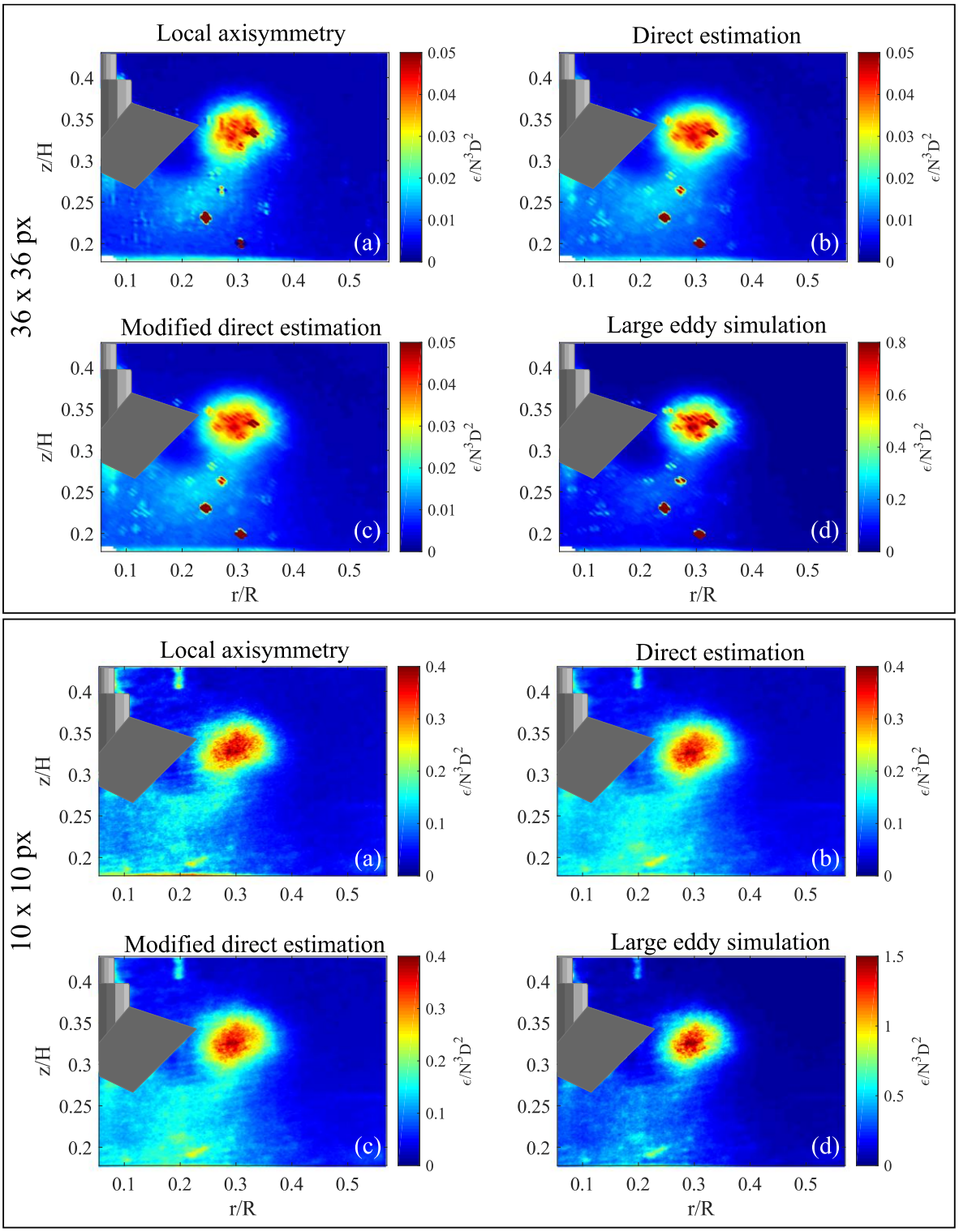

Figure 3: Angle-resolved EDR distribution of 45° using different estimation methods with 36 × 36 px or 10 × 10 px: (a) AS; (b) DE; (c) MDE and (d) LES.

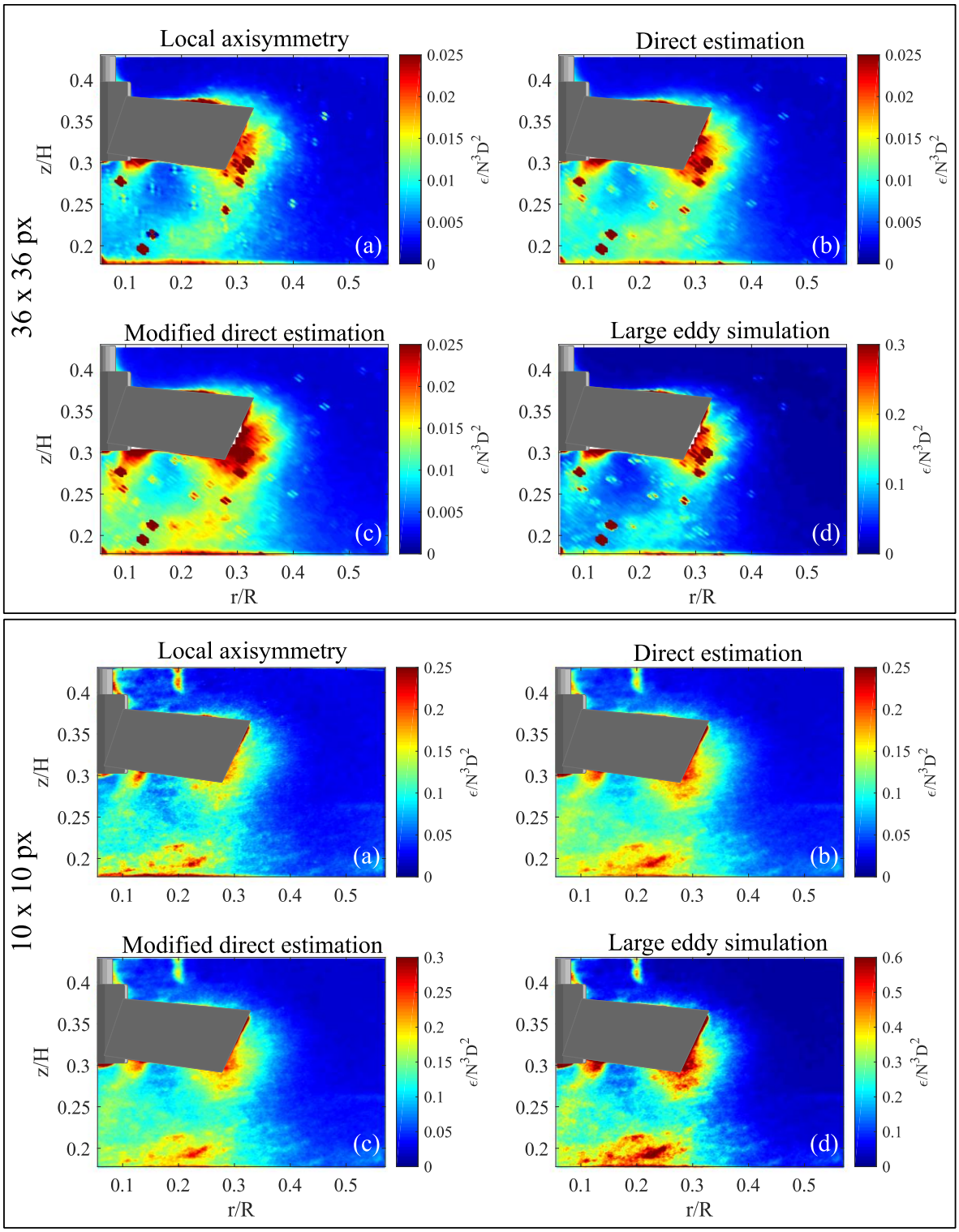

Figure 4: Angle-resolved EDR distribution of 75° using different estimation methods with 36 × 36 px or 10 × 10 px: (a) AS; (b) DE; (c) MDE and (d) LES.

According to Saarenrinne *et al.* (2001), it is possible to obtain 90% accuracy in determining the EDR for $\Delta \approx 2\eta$ and 65% accuracy for $\Delta \approx 9\eta$. In this work, η = 0.029 mm determined by $\eta = (\upsilon^3/\bar{\varepsilon}_T)^{1/4}$. The average rate of energy dissipation in the tank was obtained by $\varepsilon = \bar{\varepsilon}_T = P/\rho V$. In this case, P ($P = 2\pi MN$) is the power, M being the torque (0.98952 $N \cdot m$), obtained experimentally for 660 rpm, and V the tank volume (0.05 m^3). Thus, for the spatial resolution of 36 × 36 px, we obtained $\Delta \approx 37\eta$, which was equivalent to an accuracy of 8% for EDR. And for the spatial resolution of 10 × 10 px, the calculated value was $\Delta \approx 10\eta$, which was a representation close to 50% for the EDR distribution. Figure 5 shows the results for the mean spatial dissipation obtained as a function of the interrogation window for the 0°,

45°, and 75° plane. The results showed an exponential effect of the EDR values with the decrease in Δ that confirms which was already reported in the literature. As shown in Fig. 6, decreasing to a resolution of 5 × 5 px (Δ = 0.15 mm) for AR 45°, the noise interference became predominant due to several factors in PIV measurements. Some of them can be the possible insufficiency of pairs of images of correlated particles, reflections of the laser light, particle diameter very close to the value of Δ, among others (Tanaka e Eaton, 2007). In this way, the values of the EDR distribution were overestimated at this resolution.

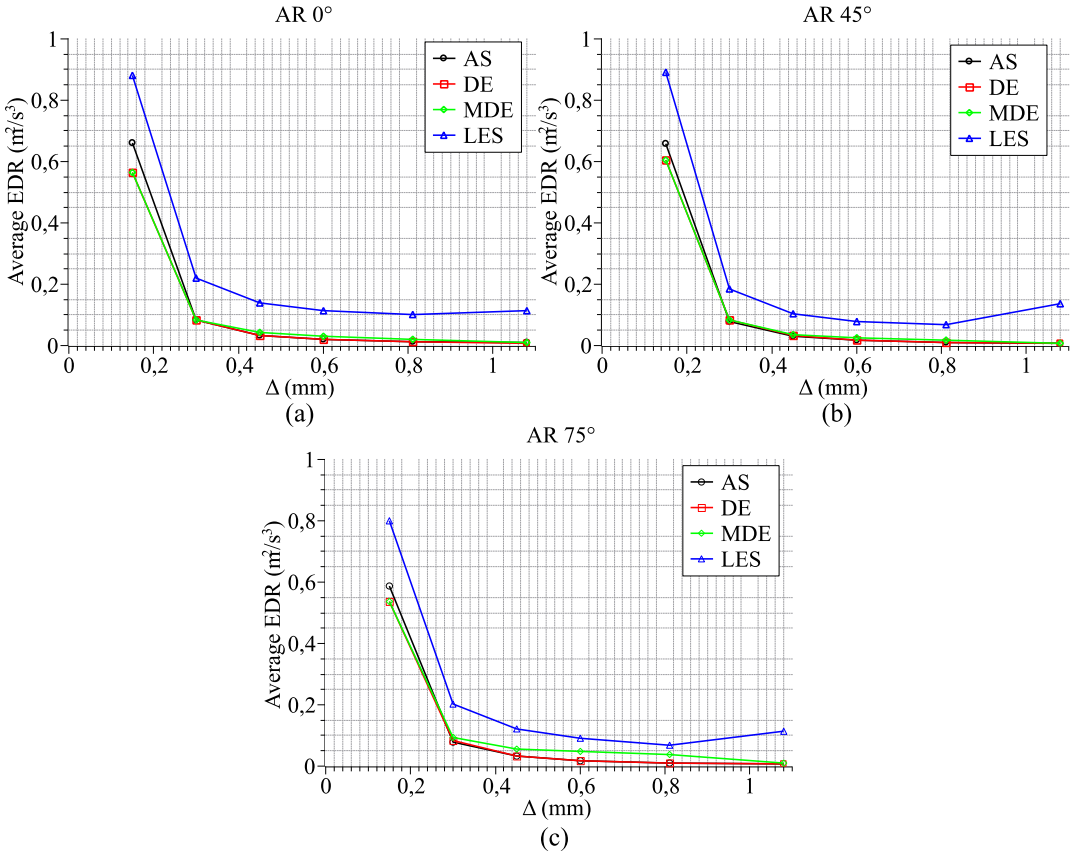

Figure 5: Turbulence energy dissipation, averaged over the impeller stream region, plotted against spatial resolution of the PIV measurements (a) AR 0°, (b) AR 45°, (c) AR 75°.

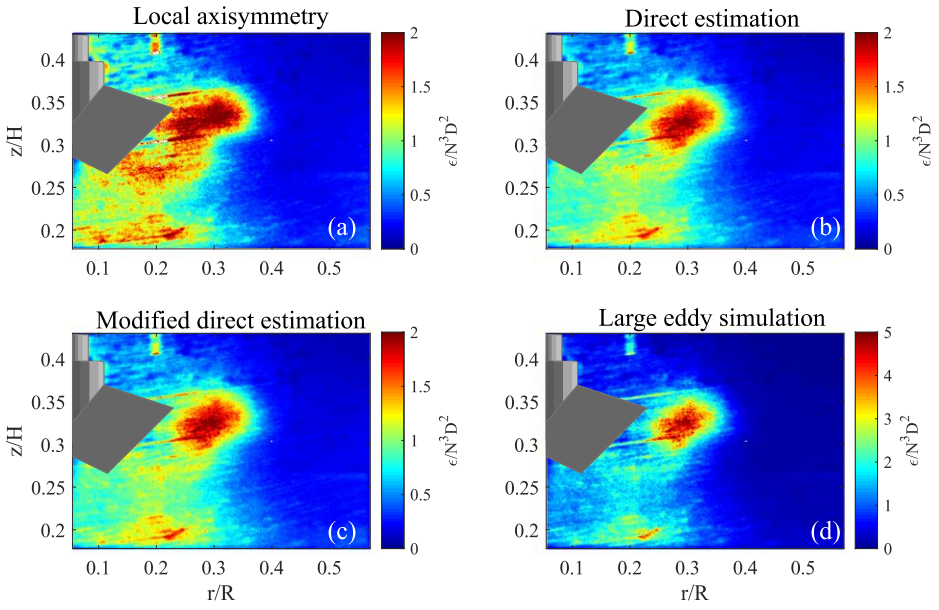

Figure 6: Angle-resolved EDR distribution of 45° using different estimation methods with 5 × 5 px (0.15 mm): (a) AS; (b) DE; (c) MDE and (d) LES.

Direct estimation of EDR using velocity gradients with the assumption of isotropy (DE), local axisymmetry (AS), or local isotropy (MDE) resulted in a significant underestimation of EDR with the growth of Δ. However, the indirect estimate (LES) showed higher values of EDR compared to the other methods, although it showed the same variation with the increase in Δ. The DE and AS methods showed subtle differences for EDR (Fig. 5), but the values were underestimated due to the hypotheses followed by the methods. For example, the assumption of the isotropy that approximates seven components of the velocity gradient tensor making the precision of the DE method difficult, since the small-scale flow is anisotropic, not only near the impeller tip but throughout the all investigated region (Sharp and Adrian, 2001). In addition to the isotropy assumption, the numerical error in the estimation of the velocity gradient from the PIV data increases the susceptibility of the presence of noisy data (Hoque *et al.*, 2015). To apply the AS method, the axisymmetric axis must be predetermined, and different selections result in differences in the EDR, and as the DE method, it provides significant underestimated values as the size of the interrogation window increases (Xu and Chen, 2013).

Regarding the MDE method, the Pao (1965) model was used to evaluate the results obtained. Figure 7 (a) shows, for example, for AR 45°, that the data obtained from the spatial resolution of 36 × 36 px not fitted the model presented, unlike the data obtained from the spatial resolution of 10 × 10 px (Fig. 7 (b)) that converged reasonably – see region $30 < \Delta/\eta < 250$. Thus, it is possible to assume that the MDE model has little influence to correct the underestimation of EDR.

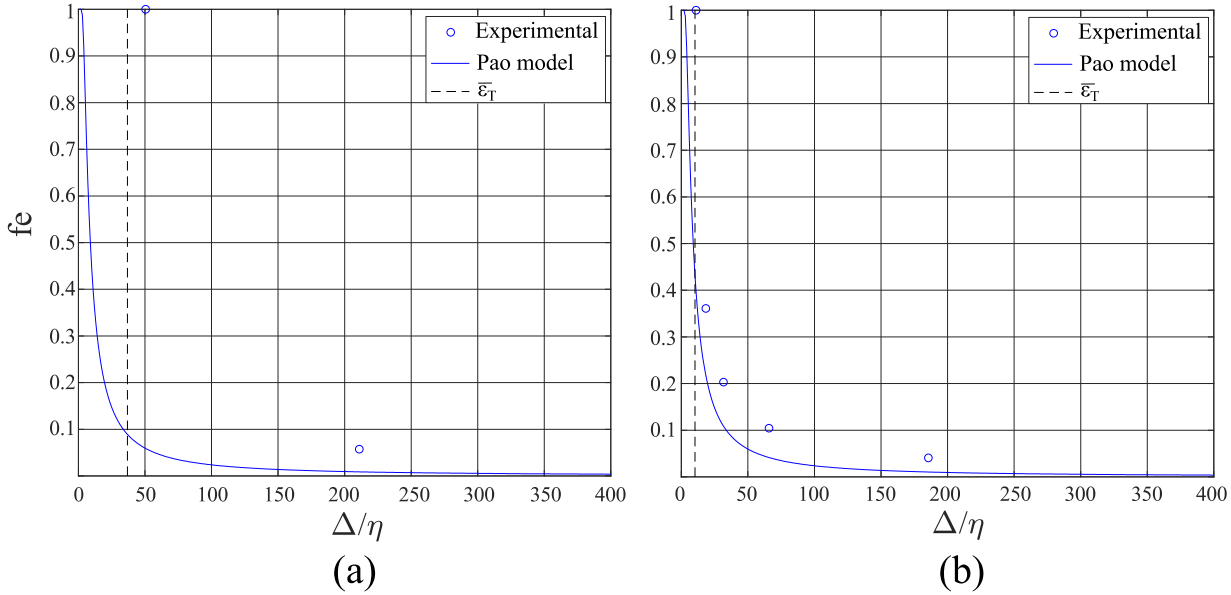

Figure 7: The underestimation coefficients (f_e) for EDR using MDE with (a) 36 × 36 px (1.08 mm) and (b) 10 × 10 px (0.3 mm).

Based on an LES approach, the EDR captures at least 70% of the real value of the kinetic energy dissipation in the flow using PIV (Sharp and Adrian, 2001). The LES method estimates the dissipation rates using a simple turbulent viscosity hypothesis model. As shown in Fig. 2, the values obtained for EDR by the LES method are higher than the DE, MDE, and AS methods. Since the current PIV measurements were not resolved to the Kolmogorov scale, the Smagorinsky model was used to estimate the amount of dissipation contained in the unresolved scales. Thus, this method is dependent on the Smagorinsky constant, and according to Meyers and Sagaut (2007) the theoretical behavior of C_s in many practical simulations is far from being constant. In this work, $C_s = 0.21$ was adopted as previously presented. In the literature, the value of the Smagorinsky constant generally varies between 0.13 (Gabriele *et al.*, 2009), 0.17 (Sheng *et al.*, 2000; Pope, 2000), and 0.21 (Meyers and Sagaut, 2007; Sharp and Adrian, 2001). The implementation of other values for C_s will be discussed in future work.

4. CONCLUSION

Measurements of energy dissipation rate (EDR) were obtained in a tank mechanically agitated with water by a PBT 45° impeller in downward pumping equipped with baffles using PIV (2C-2D) technique. Measurements at angle-resolved were evaluated regarding the respective impeller angles at 0°, 45°, and 75°. Four different methods for calculating the EDR were used: local axisymmetry (AS), direct estimation (DE), modified direct estimation (MDE), and large eddy simulation method (LES). Results of normalized EDR distribution showed a strong influence on the effect of spatial resolution. For the finer spatial resolution, 5 × 5 px, it was observed an overestimation of EDR levels causing loss of coherence of the dissipation phenomenon. For all angle-resolved, the deviations from the maximum values found for normalized EDR were above 80% for the AS, DE, and MDE methods. Only for the LES method, a deviation of less than

50% for the angles of 0°, 45°, and 75° was obtained.

5. ACKNOWLEDGEMENTS

This research was funded by Petroleo Brasileiro S/A – PETROBRAS (Cenpes) through Grant 2017/00376-1. The authors wish to acknowledge useful assistance and discussions concerning experimental data with the members of the Multiphase Flow Characterization Laboratory (LACEM) at the School of Chemical Engineering, University of Campinas, Brazil.

6. REFERENCES

Alekseenko, S.V., Bilsky, A.V., Dulin, V.M. and Markovich, D.M., 2007. "Experimental study of an impinging jet with different swirl rates". *International Journal of Heat and Fluid Flow*, v. 28, p. 1340-1359.

Basavarajappa, M., Draper, T., Toth, P., Ring, T.A. and Miskovic, S., 2015. "Numerical and experimental investigation of single phase flow characteristics in stirred tank using Rushton turbine and flotation impeller". *Minerals Engineering*, v. 83, p. 156-167.

Delafosse, A., Collignon, M.L., Crine, M. and Toye, D., 2011. "Estimation of the turbulent kinetic energy dissipation rate from 2D-PIV measurements in a vessel stirred by an axial Mixel TTP impeller". *Chemical Engineering Science*, v. 66, p. 1728-1737.

Ducci, A. and Yianneskis, M., 2007. "Vortex Tracking and Mixing Enhancement in Stirred Processes". *AIChE Journal*, v. 53, p. 305–315.

Escudié, R., Liné, A., 2003. "Experimental analysis of hydrodynamics in a radially agitated tank". *AlChE Journal*, v. 49, n. 3, p. 585-603.

Gabriele, A., Nienow, A.W. and Simmons, M.J.H., 2009. "Use of angle resolved PIV to estimate local specific energy dissipation rates for up- and down-pumping pitched blade agitators in a stirred tank". *Chemical Engineering Science*, v. 64, p. 126-143.

George, W.K. and Hussein, H.J., 1991. "Locally axisymmetric turbulence". *J. Fluid Mech.*, v. 233, p. 1-23.

Guida, A., Nienow A.W. and Barigou M., 2010. "The effects of the azimuthal position of the measurement plane on the flow parameters determined by PIV within a stirred vessel". *Chemical Engineering Science*, v. 65, p. 2454-2463.

Hasal, P., Jahoda, M. and Fořt, I., 2008. "Macro-instability: A chaotic flow component in stirred tanks". *Philosophical Transactions of the Royal Society A: Mathematical, Physical and Engineering Sciences*, v. 366, p. 409–418.

Hlawitschka, M.W. and Bart, H.-J., 2012. "Determination of local velocity, energy dissipation and phase fraction with LIF- and PIV-measurement in a Kuhni miniplant extraction column". *Chemical Engineering Science*, v. 69, n. 1, p. 138-145.

Hoque, M.M., Sathe, M.J., Joshi, J.B. and Evans, G.M., 2014. "Analysis of turbulence energy spectrum by using particle image velocimetry". *Procedia Engineering*, v. 90, p. 320-326.

Hoque, M.M., Sathe, M.J., Mitra, S., Joshi, J.B. and Evans, G.M., 2015. "Comparison of specific energy dissipation rate calculation methodologies utilising 2D PIV velocity measurement". *Chemical Engineering Science*, v. 137, p. 752-767.

Joshi, J.B., Nere, N.K., Rane, C.V., Murthy, B.N., Mathpati, C.S., Patwardhan, A.W. and Ranade, V.V., 2011. "CFD Simulation of stirred tanks: Comparison of turbulence models. Part I: Radial flow impellers". *The Canadian Journal of Chemical Engineering*, v. 89, p. 23-82.

Khan, F.R., 2005. *Investigation of turbulent flows and instabilities in a stirred vessel using a particle image velocimetry*. Ph.D. thesis, Loughborough University, Loughborough.

Kim B.J. and Sung H.J., 2006. "A further assessment of interpolation schemes for window deformation in PIV". *Experiments in Fluids*, v. 41, p. 499–511.

Liu, N., Wang, W., Han, J., Zhang, M., Angeli, P., Wu, C., Gong, J., 2016. "A PIV investigation of the effect of disperse phase fraction on the turbulence characteristics of liquid-liquid mixing in a stirred tank". *Chemical Engineering Science*, v. 152, p. 528-546.

Meyers, J. and Sagaut, P., 2007. "On the model coefficients for the standard and the variational multi-scale Smagorinsky model". *Journal of Fluid Mechanics*, v. 569, p. 287-319.

Micheletti, M., Baldi, S., Yeoh, S.L., Ducci, A., Papadakis, G., Lee, K.C. and Yianneskis, M., 2004. "On spatial and temporal variations and estimates of energy dissipation in stirred reactors". *Chemical Engineering Research and Design*, v. 82, p. 1188–1198.

Nikiforaki, L., Montante, G., Lee, K.C. and Yianneskis, M., 2003. "On the origin, frequency and magnitude of macro-instabilities of the flows in stirred vessels". *Chemical Engineering Science*, v. 58, p. 2937–2949.

Okamoto, K., Nishio, S., Kobayashi, T., Saga, T. and Takehara, K., 2000. "Evaluation of the 3D-PIV standard images (PIV-STD Project)". *Journal of Visualization*, v. 3, n. 2, p. 115-123.

Pao, Y.H., 1965. "Structure of turbulent velocity and scalar fields at large wavenumbers". *Physics of Fluids.* v. 8, p. 1063–1075.

Pope, S.B., 2000. *Turbulent Flows*. Cambridge University Press, Cambridge, New York.
Prasad, A.K., 2000. "Particle image velocimetry". *Current Science*, v. 79, n. 1, p. 51-60.
Roy, S., Acharya, S. and Cloeter, M.D., 2010. "Flow structure and the effect of macro-instabilities in a pitched-blade stirred tank". *Chemical Engineering Science*, v. 65, p. 3009–3024.
Saarenrinne, P.; Piirto, M.; Eloranta, H., 2001. "Experiences of turbulence measurement with PIV". *Meas. Sci. Technol.*, v. 12, n. 11, p. 1904-1910.
Schäfer, M., Yianneskis, M., Wächter, P. and Durst, F., 1998. "Trailing vortices around a 45° pitched-blade impeller". *AIChE Journal*, v. 44, p. 1233–1246.
Sharp, K.V. and Adrian, R.J., 2001. "PIV study of small-scale flow structure around a Rushton turbine". *AIChE J*., v. 47, p. 766-778.
Sheng, J., Meng, H. and Fox, R.O., 2000. "A large eddy PIV method for turbulence dissipation rate estimation". *Chemical Engineering Science*, v. 55, n. 20, p. 4423-4434.
Sossa-Echeverria, J. and Taghipour, F., 2015. "Computational simulation of mixing flow of shear thinning non-Newtonian fluids with various impellers in a stirred tank". *Chemical Engineering and Processing: Process Intensification*, v. 93, p. 66-78.
Tanaka, T. and Eaton, J.K., 2007. "A correction method for measuring turbulence kinetic energy dissipation rate by PIV". *Experiments in Fluids*, v. 42, p. 893–902.
Unadkat, H., 2009. *Investigation of turbulence modulation in solid-liquid suspensions using FPIV and micromixing experiments*. Ph.D. thesis, Loughborough University, Loughborough.
Westerweel, J., Elsinga, G.E. and Adrian, R.J., 2013. "Particle image velocimetry for complex and turbulent flows". *Annu. Rev. Fluid Mech.*, v. 45, p. 409-436.
Xu, D. and Chen, J., 2013. "Accurate estimate of turbulent dissipation rate using PIV data". *Experimental Thermal and Fluid Science*, v. 44, p. 662-672.
Xue, Z., Charonko, J.J. and Vlachos, P.P., 2014. "Particle image velocimetry correlation signal-to-noise ratio metrics and measurement uncertainty quantification". *Measurement Science and Technology*, v. 25, p. 1-15.
Yianneskis, M., 2000. "Trailing vortex, mean flow and turbulence modification through impeller blade design in stirred reactors". In *Proceedings of the* 10th European Conference on Mixing. Delft, The Netherlands.

7. RESPONSIBILITY NOTICE

The authors are the only responsible for the printed material included in this paper.